Modeling Water Penetration through Cracks in Waste Packages with Impinging Droplets

C.K. Ho
Sandia National Laboratories
P.O. Box 5800, Albuquerque, NM 87185-0735
U.S.A.

Z.P. Walton
Apogen Technologies
141 Leesburg Lane, Idaho Falls, ID 83404
U.S.A.

ABSTRACT

Static and dynamic models were developed to characterize and predict the hydraulic behavior in cracks in waste packages and drip shields for Yucca Mountain performance-assessment applications. A static model was developed to characterize the crack aperture based on steady, pressurized flow through the crack. Models were also developed to assess the range of apertures that would allow breakthrough of water during both static (ponded water) and dynamic (dripping) conditions. Parameters such as temperature, contact angle, and drip height were also evaluated. For static conditions, results showed that the maximum head sustainable decreased as a function of aperture. Temperature and pendant droplet size had little effect on the maximum head relative to the range of aperture sizes considered. A dynamic model was developed to evaluate the impact of crack aperture, drip height, and contact angle on the potential penetration of water through cracks with impinging water droplets. Results showed that the net downward force caused by the droplets increased as the aperture increased. The drip height and the contact angle were also found to impact the potential for penetration. For low drip heights (0.4 m), the onset of flow through cracks was predicted to occur when the crack aperture was between approximately 20 microns and 200 microns. At high drip heights (2.2 m), the onset of flow through cracks was predicted to occur when the crack aperture was between approximately 10 microns and 60 microns.

INTRODUCTION

As part of the planned engineered barrier system for the proposed high-level radioactive waste repository at Yucca Mountain, drip shields will be used to protect waste-package containers from water that may drip from the crown of the drift. Water that condenses on the underside of the drip shields may also drip onto the waste packages themselves. The potential for dripping water to penetrate cracks in the drip shield and waste-package container is the subject of this study. The amount of water that contacts the waste packages impacts performance-assessment models of corrosion and radionuclide transport within and away from the waste packages.

A literature review of studies relevant to flow through cracks or channels was conducted, but results showed that the configuration investigated in this paper is quite unique. Very little work has been performed in the past that is directly applicable to impinging droplets that may initiate flow through cracks. Therefore, static and dynamic models are developed in this paper to

characterize the potential for water to flow through cracks under static and dynamic (impinging) conditions. The intent of these modeling studies is to help guide and interpret experimental tests being conducted to characterize flow through stress-corrosion cracks.

STATIC MODELS

Two static models were developed in this study. The first static model predicts the maximum head of water that can be sustained in a crack with consideration of different fluid properties and geometric configurations. The second static model provides estimates of crack apertures based on the steady flow of water through the crack caused by a static external pressure.

Maximum Head of Water in Cracks

A static model was developed to investigates the maximum amount of water that can be supported in a crack under quiescent conditions (no external impact forces caused by impinging droplets). The amount of water that can be supported in a crack depends on the surface tension (which is a function of temperature and composition), aperture of the crack, and contact angle (wettability). A force balance can be derived based on these parameters and the opposing forces of gravity and surface tension (Figure 1). Numerous articles and fluid-mechanics text books have provided examples of this derivation for capillary tubes (e.g., [1]). However, these derivations assume that the column of water being supported is uniform. In the present configuration, the pendant droplet emerging from the bottom of the crack will tend to grow beyond the aperture of the crack. Therefore, the maximum head of water that can be supported in a crack may be less than that predicted by capillary-rise theory. The following derivation of the maximum head of water that can be supported in a crack includes the weight of a pendant droplet that is potentially larger than the crack aperture.

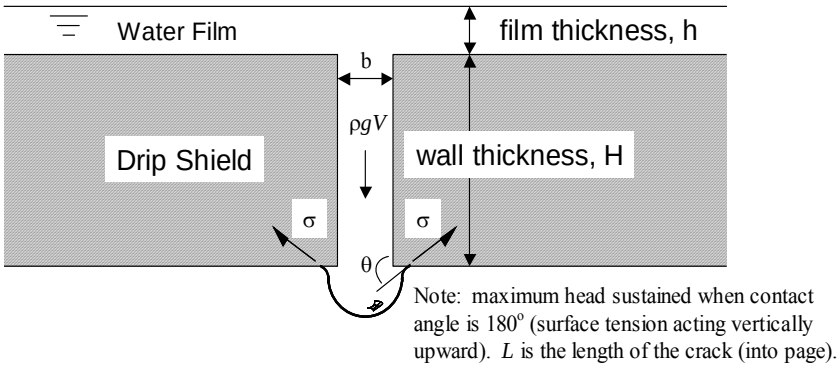

Figure 1. Schematic of a fluid-filled crack and the balance of gravity and surface-tension forces.

The weight of the water in and above the crack shown in Figure 1 is balanced by the upward force caused by the surface tension of water, as expressed in the following force balance:

$$\rho g\left(\frac{\pi D^3}{6}+Db(H+h)\right)=\sigma\pi D\left(-\cos\theta\right),\quad 90^\circ\le\theta\le 180^\circ \tag{1}$$

where H is the wall thickness (m), h is the height of the film or water column above the crack (m), D is the diameter of the pendant water droplet (m), σ is the water surface tension (N/m), θ is the contact angle relative to the vertical surface of the crack wall (degrees), ρ is the liquid water density (1000 kg/m^3), g is the gravitational constant (9.81 m/s^2), and b is the crack aperture (m).

The first term on the left-hand side of Eq. (1) represents the weight of the pendant water droplet, and the second term on the left-hand side represent the weight of the water directly above the water droplet in and above the crack. The term on the right-hand side of Eq. (1) represents the opposing upward surface-tension force along the perimeter of the water droplet. The maximum head of water that can be supported in this configuration is determined by solving for (H + h) in Eq. (1):

$$Maximum\ Head = H + h = -\frac{\pi}{b}\left(\frac{\sigma\cos\theta}{\rho g} + \frac{D^2}{6}\right), \quad 90° \le \theta \le 180° \tag{2}$$

Figure 2 shows plots of the maximum head as a function of aperture for different temperatures, droplet diameters, and contact angles. The maximum head decreases as a function of aperture. As the aperture increases, the volume of water (and its weight) increases relative to the opposing surface tension. The left plot in Figure 2 shows that temperature has little effect on the maximum head. Surface tension varies by less than 20% between 20 and 90 ºC (0.073 N/m and 0.061 N/m, respectively) [2]. In addition, the impact of droplet size, D, is small relative to the possible range of aperture sizes. The left plot in Figure 2 shows that when the droplet size is assumed to be equal to the crack aperture, b, the predicted results are similar to those when the droplet size is assumed to be equal to a constant 3.5 mm (an approximate size for a fully-developed pendant droplet). The right plot in Figure 2 shows that as the contact angle is reduced, the maximum head is also reduced because the upward force from surface tension decreases (see Figure 1). For a 0.01 mm (10 micron) aperture, the maximum head is reduced from approximately 1000 mm at a maximum contact angle of 180º to approximately 100 mm at a contact angle of 95º. The equivalent pressure in pounds per square inch for these two head values is approximately 2 psi and 0.2 psi, respectively.

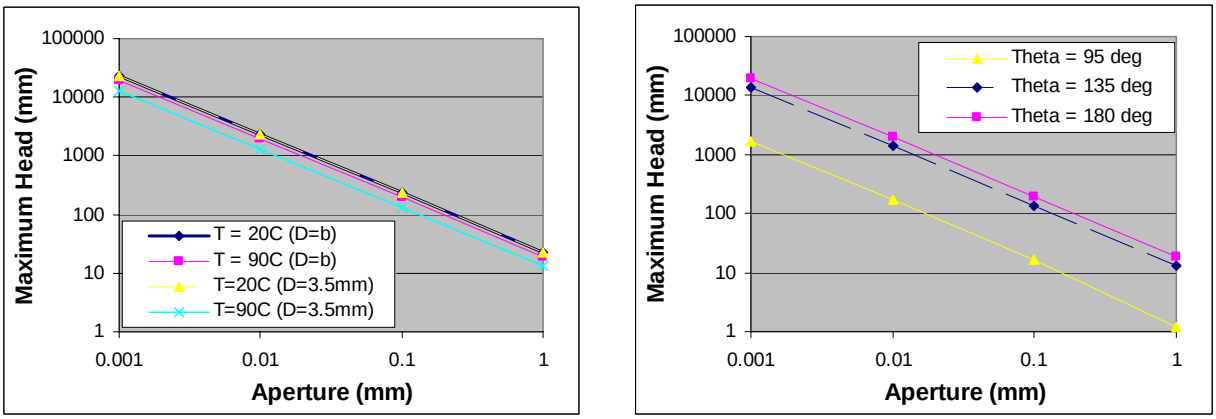

Figure 2. Maximum head as a function of crack aperture. Left: Impact of two different temperatures and droplet diameters with a contact angle of 180º. Right: Impact of different contact angles at 90 ºC with a droplet diameter (*D*) equal to the crack aperture (*b*).

Estimation of Crack Aperture

Static-pressure models were developed to estimate the effective crack aperture for steady, laminar flow through a crack with an imposed pressure gradient. These models and methods are useful to characterize effective apertures of cracks with ill-defined apertures. The equation describing steady, fully-developed, laminar flow between two plates is given as follows [1]:

$$Q = \frac{Ab^2}{12\mu}\frac{dP}{dx} \tag{3}$$

where Q is flow rate [m^3/s], A is the cross-sectional area [m^2] of the crack (aperture, b, times crack length, L), μ is the dynamic viscosity [N-s/m^2], and dP/dx is the pressure gradient across the crack. If the applied pressure is constant (and significantly greater than the pressure head of the water column), the pressure gradient can be expressed as a function of the pressure difference across the crack, ΔP [Pa], and the height of the crack, H [m]:

$$\frac{dP}{dx} = \frac{P_2 - P_0}{H} = \frac{\Delta P}{H} \tag{4}$$

The flow rate can be expressed as a function of the change in mass, Δm [kg], that is recorded gravimetrically at specified time intervals, Δt [s]:

$$Q = \frac{\Delta m}{\rho \Delta t} \tag{5}$$

Equation (1) can then be rewritten to solve for the crack aperture, b:

$$b = \left(\frac{12\mu}{\rho L}\frac{\Delta m}{\Delta t}\frac{H}{\Delta P} \right)^{1/3} \tag{6}$$

To test this model, known apertures created between two machined block samples were compared against model predictions using steady-flow test data. A constant-head apparatus was created by sealing a section of a graduated cylinder against the top of the machined-block aperture with a flange and clamps. Water was added to the cylinder until approximately 1-2 cm of head existed above the crack. Pressure was then applied to the top of the water via a pressurized nitrogen cylinder. The applied pressure (~1380-34,500 Pa or 0.2-5.0 psig) was much greater than the maximum pressure head (~300 Pa or 0.04 psig) of the water in the column, so we assume that the pressure at the entrance of the crack was equal to the applied pressure. After pressure was applied, the flow rate of water through the crack was recorded by collecting and weighing the water dripping from the crack.

Data were collected using the method described above for 0.625 mm (5/8") thick stainless-steel plates separated by shim stock. Figure 3 shows the measured flow rate and estimated aperture for cracks created with shim stock thicknesses of 25.4 and 102 microns. The accumulated mass, which represents the flow rate, is linear with time. This indicates that the applied pressure and

resulting flow rate reach a steady condition, as required by the model. After an initial transient in the beginning of the test, the predicted apertures asymptotically reach a steady value. Predicted apertures are approximately 10% higher than the actual apertures (25.4 and 102 microns) using the models and methods presented above. Therefore, the use of this model with static-head tests should provide reasonable estimates of effective apertures in cracks such as those produced by stress corrosion.

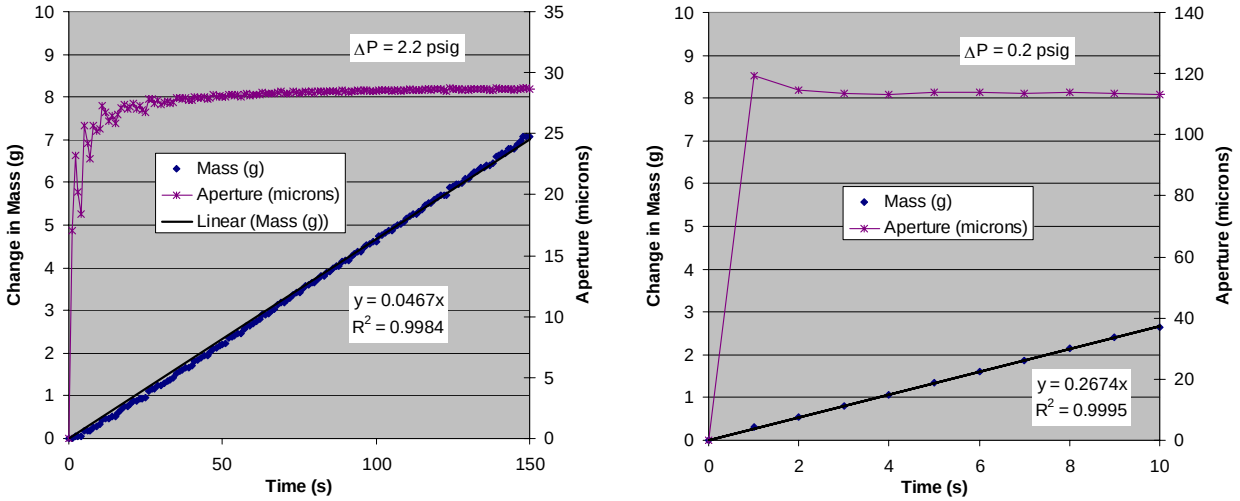

Figure 3. Measured flow rate (mass of water dripping from the crack) and estimated aperture for a constant-head experiment with a crack created using shim stock. Left: 25.4 micron shim stock. Right: 102 micron shim stock.

DYNAMIC MODEL: INITIATION OF FLOW THROUGH CRACKS BY DRIPPING WATER

Water can drip from fractures along the crown of the drift onto the drip shields below. Water that condenses on the underside of the drip shields can also drip onto the waste packages covered by the drip shields. Water that drips on top of a fluid-filled crack creates an additional downward impact force (F_i). Together with the gravity force (F_g) described in the previous section, these downward-acting forces oppose the upward-acting surface-tension force (F_s) and the viscous force (F_v). Deng [3] presented a derivation that predicts the average flow rate through cracks during an impulsive force caused by a falling droplet. This paper follows a similar derivation, but focuses on *when* flow will be initiated in cracks with impinging droplets (e.g., what aperture sizes and drip heights will initiate flow?).

Newton's Second Law can be written to determine the rate of change of the spatially averaged downward velocity, u_{ave}, in the crack in terms of the applied forces (denoted as positive downward):

$$F_g + F_i - F_s - F_v = m_{crack}\, du_{ave}/dt \qquad (7)$$

where m_{crack} is the mass of water in the crack (ρbHL). The sections below derive each of the forces in Equation (7).

The gravity force (F_g) is equal to the mass of water held in the crack times the gravitational acceleration. The mass of the film of water that may exist above the crack is neglected. Also, based on results of the static modeling of maximum head, the formation of a pendant droplet beneath the crack is neglected. The force balance yields the following equation:

$$F_g = \rho g b L H \tag{8}$$

The impact force, F_i, is determine using energy methods. The maximum potential energy per unit volume of a water drop falling from a height, l, is equal to $\rho g l$ [N/m^2]. Assuming that all of this potential energy is transferred to the impinged surfaced, the maximum total impact force, $F_{i,total}$ is equal to the area of impact times the maximum pressure, P_{max}, imparted by the falling droplet. Based on energy conservation, the maximum pressure imparted by the falling droplet is equal to initial potential energy per unit volume of the droplet (before it falls). The maximum total impact force can then be written as follows:

$$F_{i,total} = A_{impact}\, P_{max} = A_{impact}\, \rho g l \tag{9}$$

The area of impact is defined by the diameter of the water drop, D, which can be much greater than the crack aperture. Since we are only interested in the force transmitted to the liquid in the crack, we use the area of the crack, $b \cdot D$, (bounded by the diameter of the water drop) as the impact area in Equation (9) to derive an expression for the impact force, F_i, on the liquid in the crack:

$$F_i = b D \rho g l \tag{10}$$

The surface-tension force was described in the previous section and can be written as follows (assuming that the surface tension is produced along the entire length of the crack as opposed to the perimeter of a single pendant droplet):

$$F_s = -2\sigma L \cos(\theta), \quad 90^\circ \le \theta \le 180^\circ \tag{11}$$

The viscous force is caused by the shear stress (τ) of the fluid along the crack walls when flow is initiated:

$$F_v = A\tau = A\mu (du/dy)_{y=0} \tag{12}$$

where μ is the dynamic viscosity (N-s/m^2) of water, u is the downward velocity (m/s) along a horizontal cross-section of the crack, y is the horizontal distance (m) across the crack starting at the wall, and A is the area of the two walls in contact with the fluid ($2 \cdot H \cdot L$). Assuming that the flow in the crack is laminar and fully developed, the velocity profile ($u(y)$) can be derived as a function of the aperture, b, and the imposed pressure gradient along the downward direction (dp/dz):

$$u(y) = \frac{1}{2\mu}\frac{dp}{dz}\left(y^2 - by\right) \tag{13}$$

The derivative of the velocity with respect to *y* can be evaluated at *y*=0 (along the wall), yielding the following expression for the viscous force:

$$F_v = -bHL(dp/dz) \tag{14}$$

The pressure gradient can be written in terms of the average crack velocity (u_{ave}), which can be calculated by integrating Equation (13) with respect to *y* from *y*=0 to *b* and dividing by the aperture, *b*:

$$u_{ave} = -\frac{b^2}{12\mu}\frac{dp}{dz} \tag{15}$$

Solving for *dp/dz* in Equation (15) and substituting the resulting expression into Equation (14) yields the following equation for the viscous force:

» $$F_v = 12\mu \cdot H \cdot L \cdot u_{ave}/b \tag{16}$$

Note that the viscous force depends on the crack velocity, u_{ave}. Newton's 2nd Law (Equation (7)) can then be written as follows:

$$\alpha - \beta u_{ave} = du_{ave}/dt \tag{17}$$

where $$\alpha = g + \frac{glD}{HL} - \frac{-2\sigma\cos\theta}{\rho bH} \tag{18}$$

$$\beta = \frac{12\mu}{\rho b^2} \tag{19}$$

Equation (17) can be separated and integrated to yield the following expression:

$$\int_0^t dt = t = \int_0^{u_{ave}(t)} \frac{du_{ave}}{\alpha - \beta u_{ave}} = -\frac{1}{\beta}\ln\left(1 - \frac{\beta}{\alpha}u_{ave}(t)\right) \tag{20}$$

Equation (20) can be solved in terms of the time-dependent crack velocity:

$$u_{ave}(t) = \frac{\alpha}{\beta}\left[1 - \exp(-\beta t)\right] \tag{21}$$

From Equation (21), we see that a positive (downward) velocity will only occur when α is positive (i.e. when the static weight and impact forces per unit mass of water in the crack (first two terms on the right-hand side of Equation (18)) are greater than the surface tension force per unit mass of water in the crack (last term on the right-hand side of Equation (18)). Therefore, Equation (18) can be plotted as a function of crack aperture to determine when α is positive so that downward water movement can occur through the crack. It should be noted that this condition is a lower bound as a metric for water penetration. Even though movement of the water in the crack can be initiated, the total volume of water that is moved during the time of

impact (from the falling water droplet) may be insignificant. A more rigorous analysis can be conducted to calculate the volume of water expelled through the crack during the impact time by integrating Equation (21) and multiplying the result by the area of the crack. If the volume of water moved during the time of impact is less than, say, 0.1% of the total volume of water held in the crack, then it is unlikely that any water will actually be expelled from the crack.

Figure 4 shows a plot of the net downward force per unit mass of water held in the crack (α) vs. crack aperture (b) for different parameter variations. Four different parameter combinations are evaluated to investigate the impact of drip height and contact angle. Only two values (high and low) are considered for each parameter. Temperature is not included as a variable because previous results showed that the impact of temperature on surface tension was relatively small (surface tension decreases by less than 20% from 20 ºC to 90 ºC). Although the dynamic viscosity decreases significantly with an increase in temperature (by a factor of three from 1.0×10^{-3} N-s/m^2 to 3.2×10^{-4} N-s/m^2 when the temperature increases from 20 ºC to 90 ºC [1]), the dynamic viscosity does not play a role in the initiation of water movement in the crack. The parameter values for each of the high and low values used in the calculations are shown in Table 1.

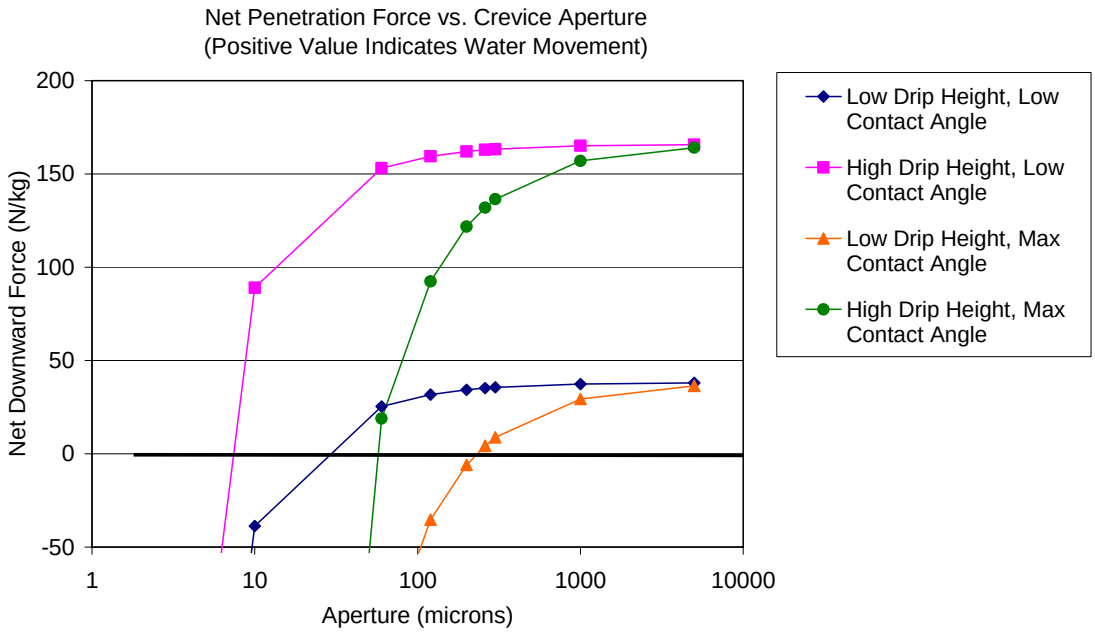

Figure 4. Predicted net downward force vs. crack aperture when a falling water droplet impinges on top of a water-filled crack. When the net downward force (gravity + impact – surface tension) is positive, downward water movement can occur in the crack.

Table 1. Parameter values for calculation of net downward force caused by a falling water droplet on a water-filled crack.

Parameter	Low Value	High Value
Drip Height (m)	0.4	2.2
Contact Angle (degrees)	95	180
Height of Crack (m)	0.0159 (0.625")	NA
Length of Crack (m)	0.0305 (1.2")	NA
Droplet diameter (m)	0.0035	NA

Figure 4 shows that the net downward force increases as the aperture increases. As the aperture increases, the downward gravity force (F_g) and impact force (F_i) transmitted to the liquid in the crack increases while the surface-tension force remains the same. The drip height and the contact angle also impact the potential for penetration. For low drip heights, the onset of flow through cracks is predicted to occur when the crack aperture is between approximately 20 microns (at a contact angle of 95 degrees) and 200 microns (at a maximum contact angle of 180 degrees). At high drip heights, the onset of flow through cracks is predicted to occur when the crack aperture is between approximately 10 microns (at a contact angle of 95 degrees) and 60 microns (at a maximum contact angle of 180 degrees).

The height and length of the crack used in the predictions were chosen based on samples that were available for testing. The actual length of a crack will be quite variable. If the length of the crack were decreased, Eq. (18) shows that the net downward force would increase and the onset of flow would occur at lower aperture sizes. However, actual cracks such as those produced by stress corrosion will be more tortuous than the uniform cracks assumed here. Non-uniform apertures and asperities not considered in this paper will likely create additional capillary barriers that delay the onset of flow in actual cracks.

CONCLUSIONS

Static and dynamic models were developed in this paper to characterize and predict flow through cracks in waste-package containers and drip shields. Static-model results showed that the maximum head of water that can be supported by surface tension decreased linearly as a function of aperture. As the aperture increased, the volume of water (and its weight) increased linearly relative to the opposing surface tension. Temperature had little effect on the maximum head, and surface tension varied by less than 20% between 20 and 90 ºC (0.073 N/m and 0.061 N/m, respectively). As the contact angle was reduced, the maximum head was also reduced because the upward force from surface tension decreased. For a 0.01 mm (10 micron) aperture, the maximum head reduced from approximately 1000 mm at a contact angle yielding maximum upward surface tension to approximately 100 mm at a contact angle yielding minimal upward surface tension.

Models of steady, laminar flow through cracks were developed to estimate the effective aperture in cracks. Comparisons to tests showed that the predicted apertures were approximately 10% greater than the actual values, ranging from 25 microns to over 100 microns. These results imply

that the models and static-pressure tests may be useful for estimating effective apertures for ill-defined cracks such as those produced by stress corrosion.

Finally, a dynamic model was developed to evaluate the impact of crack aperture, drip height, and contact angle on the potential penetration of water through cracks with impinging water droplets. Results showed that the net downward force caused by the droplets increased as the aperture increased. As the aperture increased, the downward gravity force and impact force transmitted to the liquid in the crack increased while the surface-tension force remained the same. The drip height and the contact angle were also found to impact the potential for penetration. For low drip heights (0.4 m), the onset of flow through cracks was predicted to occur when the crack aperture was between approximately 20 microns and 200 microns. At high drip heights (2.2 m), the onset of flow through cracks was predicted to occur when the crack aperture was between approximately 10 microns and 60 microns. However, tortuous pathways and asperities in actual cracks may create additional barriers that delay the onset of flow when compared to the predicted results of the idealized uniform cracks assumed here.

ACKNOWLEDGMENTS

This work was supported by the Yucca Mountain Site Characterization Office as part of the Civilian Radioactive Waste Management Program, which is managed by the U.S. Department of Energy, Yucca Mountain Site Characterization Project. Sandia is a multiprogram laboratory operated by Sandia Corporation, a Lockheed Martin Company for the United States Department of Energy's National Nuclear Security Administration under contract DE-AC04-94AL85000.

REFERENCES

1. Roberson, J.A. and C.T. Crowe (1985). *Engineering Fluid Mechanics*, 3rd Ed., Houghton Mifflin Company, Boston.
2. Lide, D.R., ed. (2002). *CRC Handbook of Chemistry and Physics*. 83rd Edition. Boca Raton.
3. Deng, (2001). Water Distribution and Removal Model, Yucca Mountain Model Report, *ANL-EBS-MD-000032 Rev. 01*, Civilian Radioactive Waste Management System Management and Operating Contractor, Las Vegas, NV.